

Evidence for Macroscopic Quantum Tunneling of Phase Slips in Long One-Dimensional Superconducting Al Wires

Fabio Altomare,^{1,2} Albert M. Chang,^{1,2} Michael R. Melloch,³ Yuguang Hong,⁴ and Charles W. Tu⁴

¹*Physics Department, Duke University, Durham, NC 27708*^{*}

²*Physics Department, Purdue University, West Lafayette, IN 47906*

³*School of Electrical and Computer Engineering, Purdue University, West Lafayette, IN 47906*

⁴*Department of Computer and Electrical Engineering, UCSD, La Jolla, CA 92093*

(Dated: December 2, 2024)

Quantum phase slips have received much attention due to their relevance to superfluids in reduced dimensions and to models of cosmic string production in the Early Universe. Their establishment in one-dimensional superconductors has remained controversial. Here we study the nonlinear voltage-current characteristics and linear resistance in long superconducting Al wires with lateral dimensions ~ 5 nm. We find that, in a magnetic field and at temperatures well below the superconducting transition, the observed behaviors can be described by the non-classical, macroscopic quantum tunneling of phase slips, and are inconsistent with the thermal-activation of phase slips.

PACS numbers: 74.78.Na, 74.25.Fy, 74.25.Ha, 74.40.+k

What is the resistance of a superconductor below its superconducting transition temperature? For a three-dimensional superconductor, the answer is the obvious one – zero. But in one-dimension (1D), by which we mean very thin very long wires, quantum fluctuations destroy the zero resistance state. Phase slips – small superconducting regions that become normal, allowing the phase of the order parameter to rapidly change by 2π – give rise to residual resistance and can even quench superconductivity completely. The tiny cross-section of 1D nanowires reduces the free energy barrier arising from a loss of condensation energy for the creation of phase slips. Thermal activation of phase slips (TAPS) across this barrier is responsible for the residual resistance just below T_c (LAMH picture) [1]. On the other hand, macroscopic quantum tunneling of phase slips (QTPS) as the source of residual resistance at low temperatures has remained controversial despite intense experimental effort [2, 3, 4, 5, 6, 7, 8]. The observation of macroscopic quantum tunneling is of significance not only for 1D superconductivity, but also for understanding the decoherence of quantum systems due to interaction with their environment. Here we clearly establish the presence of QTPS in superconducting (SC) Al nanowires, showing the dramatic effect they have on the voltage-current (V-I) characteristics of the wire.

Phase slips in 1D SC nanowires have traditionally been studied by measuring the linear resistance as a function of the temperature through the normal-superconducting (N-S) transition. Any resistance in excess to that predicted by thermal activation is attributed to macroscopic tunneling of phase slips [2, 3, 4, 5, 6, 7]. However, this attribution can be flawed because of weak links in the wire resulting from inhomogeneities [3, 7]. Moreover, the fitting of the excess residual resistance to quantum-phase-slip expressions [2, 5, 6, 7] often necessitated an ad hoc reduction in the free-energy barrier. Recently Rogachev

et al. [8] examined the nonlinear V-I dependence of $Mo_{0.79}Ge_{0.21}$ SC nanowires: they found that the deduced residual resistance, spanning 11 orders in magnitude, followed the prediction of classical TAPS alone, thus contradicting previous claims of QTPS behavior based on residual linear resistance by the same group [4, 5].

In this Letter, we examine the nonlinear V-I characteristics and linear resistance of long aluminum nanowires, the narrowest one with dimension 5.2 nm x 6.1 nm x 100 μ m (21 x 24 x 400,000 atoms). Our wires are much longer than those of similar cross section reported in the literature ($\sim 0.5\mu$ m long)[4, 5, 8] and the ratio of the low temperature SC coherence length to the width (or height) is also much larger, thus placing us in a regime distinct from previous works. Specifically, we study the residual resistance deduced from the nonlinear V-I characteristics in the superconducting state below the critical current. Our main finding is that the V-I dependence and residual resistance are inconsistent with the classical LAMH behavior, but instead are well described by quantum expressions, either derived from an extension of the classical model [2] or in a recently proposed power-law form [9, 10, 11]. The good fits to the different quantum expressions, which closely overlap each other, are corroborated by measured residual linear resistance, achieving full consistency within the quantum scenario using a single set of fitting parameters. Our results demonstrate the importance of non-classical, quantum phase slips in ultranarrow, 1D superconducting aluminum wires.

The nanowires were fabricated by thermally evaporating aluminum onto a narrow, 8 nm-wide, MBE (molecular-beam-epitaxy) grown InP ridge, while at once linking and partially covering the four-terminal Au/Ti measurement pads (Fig. 1(b)). The fabrication is described elsewhere[12]. Magnetoresistance at 4.2 K (above T_c) was used to characterize the wires (Table 1). The calculated dirty limit ξ [13] (≈ 94 nm for s1, ≈ 128 nm for

	L μm	w nm	t nm	R_N kΩ	ρ μΩcm	l_e nm	ξ nm	J_c (0.35 K) $10^5 A/cm^2$
s1	10	6.9	9.0	8.3	5.1	7.6	94	12.1
s2	100	5.25	6.09	86	2.8	14.3	128	13.1

TABLE I: Parameters for sample s1 and s2, including L (length), w (width), t (thickness), R_N (normal state resistance), ρ (resistivity), l_e (mean free path), ξ (GL coherence length), and J_c (critical current density). w , t , ρ and l_e were deduced based on magnetoresistance measurements [12]. ξ was calculated using $\xi = 0.85\sqrt{\xi_0 l_e}$ where $\xi_0 = 1600$ nm is the GL superconducting coherence length in bulk aluminum.

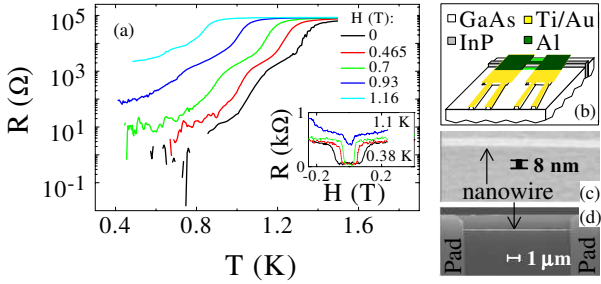


FIG. 1: (Color) (a) Linear resistance versus temperature for wire s2 in different magnetic fields; the pad series resistance has been subtracted[15]. Inset: The pad series resistance increases at magnetic fields beyond the critical field of the pad regions covered by aluminum ($T=0.38, 0.80, 0.99, 1.10$ K). (b)-(d) Schematic and SEM images of a nominally 8 nm wide Al nanowire (similar to samples s1 and s2): the Al layer does not entirely cover the Au/Ti pads which were measured in series with the superconducting wire.

s2) far exceeds the lateral dimensions ($\sim 5 - 9$ nm).

To investigate the SC behavior, the linear resistance through the N-S transition was measured at a current of 1.6 nA (Fig. 1(a)), while the nonlinear V-I characteristics was measured in both the constant-current (Figs. 2(a)-(b) and 3) and constant-voltage modes below T_c [14]. The linear resistance drops by several orders of magnitude from the normal state resistance (R_N) through T_c , but remains finite. In Fig. 1(a) we show the linear resistance versus temperature for wire s2 in different magnetic fields (H)[15]. At a given temperature, the resistance increases with increasing H as superconductivity weakens. In the constant-current mode, finite residual nonlinear voltage is observed in the V-I curves below the critical current jump. Such residual voltage is unobservable in large wires. In the constant-voltage mode, the V-I curves exhibit non-hysteretic voltage steps and S-shaped curves down to $T/T_c \approx 0.2$, typical of 1D superconductors [6, 16]. Evidences for wire homogeneity include: 1) comparable critical current density in wires s1 and s2 2) all V-I traces in the constant-current mode showed a single critical current jump.

To assess the importance of QTPS, we focus on the residual resistance and residual voltage below T_c for sample s2; the wider s1 will be used for control as discussed

below. The main datasets consist of the nonlinear V-I curves in constant-current mode (Figs. 2(a)-(b) and 3 (black curves)), and the linear resistance versus T . This latter resistance is obtained in two ways: (i) from the data in Fig. 1(a) [15] (Figs. 2(c)-(d) (black curves)), and (ii) from the fits to the nonlinear V-I curves according to Eqs. (1b) and (3) below (Δ , Figs. 2(e)-(f)). It will be demonstrated through quantitative analysis that this entire set of data is inconsistent with the TAPS scenario, as evidenced by the poor fits to the LAMH expressions (Eqs. (1a) and (1b)) shown in Figs. 2 and 3 (blue curves). Instead the inclusion of the QTPS contributions (Giordano (GIO) model Eqs. (2) and (3)) in the fits is essential in providing a fully consistent description based on a single set of parameters (see red curves in Figs. 2 and 3).

Thermal activation of phase slips, important at $T \lesssim T_c$, is well described by the expressions derived by Langer Ambegaokar, McCumber, Halperin (LAMH)[1, 17]:

$$R_{LAMH} = R_q \frac{\Omega}{k_B T} \exp\left(-\frac{\Delta F}{k_B T}\right), \quad (1a)$$

$$V_{TAPS} = I_0 R_{LAMH} \sinh(I/I_0), \quad (1b)$$

where the quantum resistance $R_q = \pi \hbar/2e^2$, attempt frequency $\Omega = (L/\xi)(\Delta F/k_B T)^{1/2}(\hbar/\tau_{GL})$, free energy barrier $\Delta F = (8\sqrt{2}/3)(H_{th}^2/8\pi)A\xi$, and Ginzburg-Landau relaxation time $\tau_{GL} = (\pi/8)[\hbar/k_B(T-T_c)]$, $I_0 = 4ek_B T/h$. L is the wire length, T the temperature, k_B the Boltzmann constant, H_{th} the thermodynamical critical field, A the wire cross section, and ξ the GL coherence length.

Quantum tunneling of phase slips, which takes place in parallel with thermal activation, is expected to dominate at low T . Giordano[2] proposed a quantum form by replacing kT with $(1/a_{GIO})(\hbar/\tau_{GL})$ [17, 18]:

$$R_{GIO} = R_q \frac{L}{\xi} \sqrt{a_{GIO} \frac{\Delta F}{\hbar/\tau_{GL}}} \exp\left(-a_{GIO} \frac{\Delta F}{\hbar/\tau_{GL}}\right) \quad (2)$$

where a_{GIO} is a numerical constant of order unity and, in analogy with the thermal case, we propose that[17, 18]:

$$V_{QTPS} = I_{GIO} R_{GIO} \sinh(I/I_{GIO}) \quad (3)$$

where $I_{GIO} = 2e/(\pi\tau_{GL}a_{GIO})$. In this quantum case, a resistance similar to the Giordano expression (and numerically equivalent) has been recently derived, on a microscopic basis, by Golubev and Zaikin [9] and by Khlebnikov and Pryadko [10]. In the nonlinear regime, both theories predict a crossover from an exponential dependence to a power-law behavior ($V \propto I^\nu$) at low T .

To begin the analysis, we first extract the parameters, T_c and ξ at each magnetic field and a single a_{GIO} , by fitting to the linear R versus T traces in Figs. 2(c)-(d); T_c and a_{GIO} are input parameters in the analysis of the V-I curves. Below T_c , a wire is modeled as a normal and a superconducting wire in parallel, the latter with a resistance produced by the relevant phase slips mechanism[5].

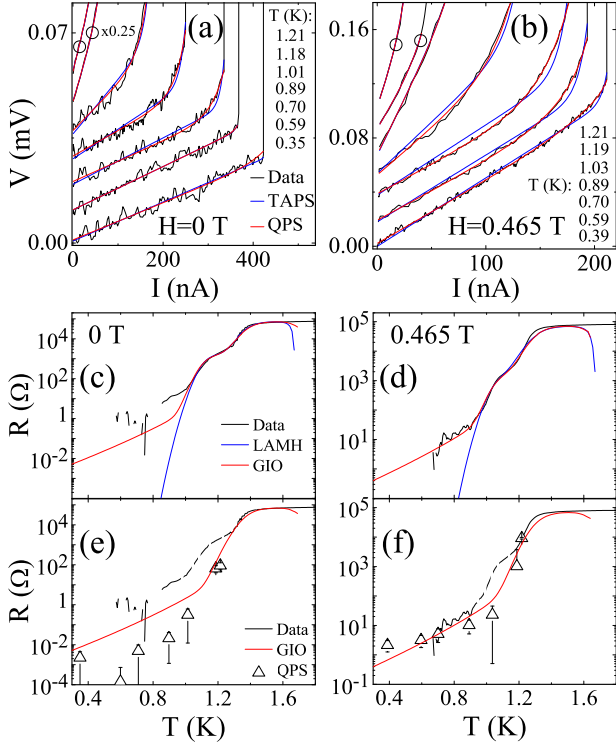


FIG. 2: (Color) Nonlinear V-I curves and linear resistance for sample s2 at different magnetic fields (H): Black curves—data; red curves—fits to the GIO (\equiv GIO + LAMH) expressions for QPS (\equiv TAPS + QTPS), and blue curves—fits to the LAMH expressions for TAPS alone. (a)-(b) V-I curves offset for clarity. The fits to QPS are of higher quality compared to TAPS; each fit includes a series resistance term V_S . These V-I curves can be fitted equally well by a power law form $V = V_S + K \cdot (I/I_k)^\nu$ where $12 \gtrsim \nu \gtrsim 3.2$ for $0 \leq H \leq 1.05$ T[10, 11]. (c)-(d) Linear resistance after background subtraction (see Fig. 1(a) and [15]). The LAMH fits are poor at low T . (e)-(f) The resistance contribution due to phase slips (R_{QPS}) extracted in (a)-(b) from fits to the V-I curves using the GIO expressions (discrete points, Δ). R_{QPS} and the linear resistance from (c)-(d) are refitted using the GIO expressions (red) with the same $a_{GIO} (= 1.2)$ while disregarding the irrelevant shoulder feature (dashed line).

To account for the shoulder feature at a resistance $\approx 1/20$ of R_N , we assume our wire to be composed of segments of two slightly different cross sectional areas, with a fixed ratio of 90% ($\Delta F \propto A$). The thinner segments corresponding to the smaller cross sectional area have a larger T_c [7]. These segments, with critical temperature (resistance) T_{c1} (R_1), are responsible for $\gtrsim 95\%$ of R_N . At zero field, the fitting parameters are $T_{c1}(H=0)$, $T_{c2}(H=0)$, $\xi(H=0)$, R_1 , and a_{GIO} , while at $H \geq 0.465$ T, only $T_{c1}(H)$, $T_{c2}(H)$, $\xi(H)$ are varied. Fitting using two ξ s produced unphysical ξ dependence on H and was discarded. The fits to the GIO (red) and LAMH (blue) theory are presented in Figs. 2(c)-(d). At $H = 0$ T both fits reproduced the data over several decades in resistance and are nearly equivalent above ≈ 5 Ω . At higher field the

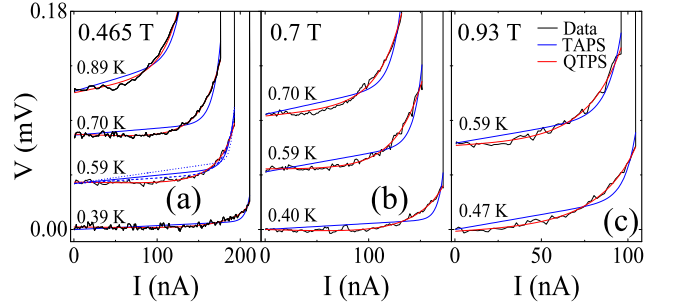


FIG. 3: (Color) The nonlinear V-I curves, at $T/T_c \lesssim 0.5$ are refitted with $V = V_{QTPS} + V_S$ and $V = V_{TAPS} + V_S$ (see text). (a)-(c) The data (black), QTPS (red) and TAPS (blue) fits and are shown after subtracting the linear background. Dotted (dashed) line in 3(a) is the fit to the TAPS expression with a 50% reduction (increase) in temperature, respectively.

GIO theory better models the data, particularly at low T [19]. The fitting parameters T_{c1} and ξ (●) are presented in Fig. 4 (a)-(b). Their H dependence can be fitted to simple theoretical expressions as shown. The single value of $a_{GIO} = 1.2$ we obtain, of order unity as expected, will be used throughout all the subsequent analysis.

Despite the success in fitting to the linear resistance, it is not possible to completely rule out weak links as the source of residual resistance. To clearly demonstrate the importance of quantum phase slips, it is necessary to analyze the nonlinear V-I dependence. Generalizing the nonlinear analysis of Rogachev et al.[8] by including QTPS while also accounting for series resistances, the total voltage drop across the superconducting nanowire is $V = V_{TAPS} + V_{QTPS} + V_S$, where V_{TAPS} and V_{QTPS} are given in Eqs. (1b) and (3), respectively[17], and $V_S = R_S I$. R_S is a series resistance which includes the contribution of the pads and other ohmic-like contributions such as proximity effect of the normal pads on the SC wire[20]. The fitting parameters are R_{TAPS} , R_{QTPS} and R_S [17], while $a_{GIO} (= 1.2)$ and $T_c(H)$, which enters through τ_{GL} , are taken from the previous fits (Fig. 4(a)). At all temperatures and fields, the fitting curves reproduce the data extremely well, as shown in red in Figs. 2(a)-(b) and 3[21]. At higher T ($T/T_c \gtrsim 0.7$) the contribution from QTPS is negligible compared to TAPS. At low T ($T/T_c \lesssim 0.5$) TAPS is expected to be exponentially suppressed (Eq. (1a)) and QTPS should dominate; this expectation is confirmed by the fits which yielded a negligible R_{TAPS} compared to R_{QTPS} [22].

To further substantiate the importance of QTPS at low T while at the same time rule out TAPS as a significant cause of phase slips, we directly compare fits of the nonlinear V-I curves using $V = V_{QTPS} + V_S$ and $V = V_{TAPS} + V_S$. The fitting parameters for QTPS are R_{QTPS} , R_S , and for TAPS they are R_{TAPS} , R_S . The curves are presented in Figs. 3(a)-(c) after subtracting the linear background for several $H > 0$ T. Although the

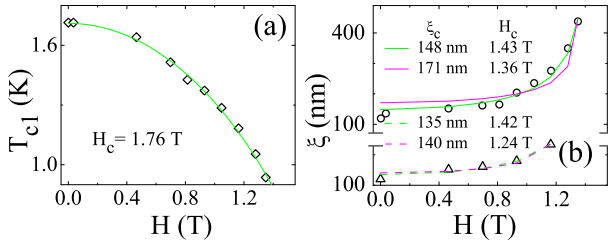


FIG. 4: (Color) GIO(\equiv GIO+LAMH) fitting parameters to the linear resistance curves, including those shown in Fig. 2(c)-(d), plotted versus H . (a) T_{c1} (\blacklozenge) and T_{c2} (not shown) fit well to the pair breaking perturbation theory[13] (green). (b) ξ (\bullet) is fitted to both $\xi = \xi_c / \sqrt{1 - (H/H_c)^2}$ (magenta) ($\Delta \propto \sqrt{1 - (H/H_c)^2}$ and $\xi \propto 1/\sqrt{\Delta}$ [13]), and to an ad hoc expression $\xi = \xi_c / \sqrt{1 - (H/H_c)^2}$ (green); $\xi_c \equiv \xi(H=0)$ and H_c is the critical field. ξ is better described by the ad hoc expression. ξ (Δ) derived from the fits to R_{QPS} , including those in Fig. 2. (e)-(f), is fitted to theory as before (dashed lines) yielding $\xi_c \approx 135$ nm, within 5% of the value in Table 1.

two expressions have the same number of parameters, the QTPS fits (red) are of good quality while the TAPS fits (blue) are evidently much poorer. Varying T by $\pm 50\%$ in the TAPS fits still failed to reproduce the data, as shown in Fig. 3(a) for $T = 0.59$ K and $H = 0.465$ T. Comparing the χ -squares of the fits that include QTPS versus TAPS alone using the statistical F-test yielded strong support for the importance of quantum phase slips with a confidence level $>99.99\%$ [23].

The $R_{QPS} = R_{QTPS} + R_{TAPS}$ extracted from the nonlinear V-I fits enables to exclude contributions to residual resistance that are irrelevant to phase slips, providing a means to check full consistency. In Figs. 2(e)-(f) we plot R_{QPS} (Δ symbols) for $T \lesssim T_c$ and replots the linear resistance through the N-S transition for comparison; we then refit the linear resistance expressions (GIO+LAMH, Eqs. (1a) + (2)) to these data, keeping $a_{GIO} = 1.2$ unaltered while varying T_c and ξ . The discrete R_{QPS} data points versus T no longer exhibit a shoulder feature, and only one T_c was needed. Satisfactory agreement is achieved as depicted in Figs. 2(e)-(f) (red). Similar agreement comparable to the $H = 0.465$ T trace is obtained at higher $H = 0.7$ T, 0.93 T, etc. T_c was essentially unchanged compared to T_{c1} in Fig. 4(a) but ξ (Fig. 4(b), Δ) was reduced at higher H , compared to the data obtained previously (Fig. 4(b), \bullet). Fitting to the new values yielded $\xi_c \equiv \xi(H=0) \approx 135$ nm, within 5% of the calculated value in Table 1. As a final consistency check, analysis of the wider superconducting sample s1[12] did not produce any sign of QTPS for $H \lesssim 0.9$ T. This is sensible because of the larger free-energy barrier.

The consistency achieved in our analysis of the nonlinear V-I curves and residual resistance, supported by the quantitative statistical F-test, demonstrates the importance of quantum phase slips. This helps rule out other

scenarios, e.g. TAPS alone or weak links. Furthermore, our results establish that the transport properties of 1D superconducting nanowires at temperatures much below T_c are determined primarily by the macroscopic quantum tunneling of phase slips. Our findings pave the way to the study of newly predicted quantum phase transitions in metallic nanowires[24].

F.A. thanks M.E. Rizza for her support. Work supported by NSF DMR-0135931 and DMR-0401648.

* Current address.

- [1] J. S. Langer and V. Ambegaokar, Physical Review **164**, 498 (1967); D. E. McCumber and B. I. Halperin, Phys. Rev. B **1**, 1054 (1970).
- [2] N. Giordano, Phys. Rev. Lett. **61**, 2137 (1988).
- [3] J. M. Duan, Phys. Rev. Lett. **74**, 5128 (1995).
- [4] A. Bezryadin *et al.*, Nature **404**, 971 (2000).
- [5] C. N. Lau *et al.*, Phys. Rev. Lett. **87**, 217003 (2001).
- [6] M. L. Tian *et al.*, Phys. Rev. B **71**, 104521 (2005).
- [7] M. Savolainen *et al.*, Appl. Phys. A **79**, 1769 (2004); M. Zgirski *et al.*, Nano Letters **5**, 1029 (2005).
- [8] A. Rogachev *et al.*, Phys. Rev. Lett. **94**, 017004 (2005).
- [9] D. S. Golubev and A. D. Zaikin, Phys. Rev. B **64**, 014504 (2001).
- [10] S. Khlebnikov and L. P. Pryadko, Phys. Rev. Lett. **95**, 107007 (2005).
- [11] EPAPS Document No. (Section 1) summarizes the magnetic field behavior of the exponent.
- [12] F. Altomare *et al.*, Appl. Phys. Lett. **86**, 172501 (2005).
- [13] Tinkham M., Introduction to Superconductivity, (1996).
- [14] Linear resistance measurements were performed with a lockin-amplifier at 23 Hz. Room temperature filters and low temperature RC filters, formed naturally from the sample lead resistances ($\approx 2-20$ k Ω) and capacitances to ground (≈ 0.5 nF), helped reduce noise to the nanowires.
- [15] See EPAPS Document No. (Section 2) .
- [16] D. Y. Vodolazov *et al.*, Phys. Rev. Lett. **91**, 157001 (2003).
- [17] To distinguish the fitting parameters from the theoretical values, we refer to R_{TAPS} (R_{QTPS}) as the TAPS (QTPS) resistance extracted from fits to the V-I, and to R_{LAMH} (R_{GIO}) as the calculated values for TAPS (QTPS).
- [18] In the following, when referring to the GIO theory, we will implicitly include the LAMH contribution as well.
- [19] At sufficiently high H -field, the rapid increase in ξ and decrease in T_{c1} reduces the free energy barrier ($\Delta F(H, T) \approx 0.83 \frac{R_q}{R_N} \frac{L}{\xi(H, T=0)} k_B T_{c1}(H) (1 - T/T_{c1}(H))^{3/2}$ [6] (Fig. 4(a)-(b)). For a *given intermediate temperature* the contribution from TAPS can actually become larger.
- [20] G. R. Boogaard *et al.*, Phys. Rev. B **69**, 220503(R) (2004).
- [21] The establishment of the nanowire electron temperature is in Section 4 of the EPAPS Document No.
- [22] For the data central to QTPS shown in Figs. 2(f) and Fig. 3, there were a total of 21 fitting parameters for 1106 data points in the 10 traces, or 53 points per parameter.
- [23] See EPAPS Document No. (Section 3) for F-test details.
- [24] S. Sachdev *et al.*, Phys. Rev. Lett. **92**, 237003 (2004).

Erratum: Non-linear Current-Voltage Dependence of the Superconducting Transition in 1-D Ultranarrow Al wires

Fabio Altomare,^{1,2} Albert M. Chang,^{1,2} Michael R. Melloch,³ Yuguang Hong,⁴ and Charles W. Tu⁴

¹*Physics Department, Duke University, Durham, NC 27708*

²*Physics Department, Purdue University, West Lafayette, IN 47906*

³*School of Electrical and Computer Engineering, Purdue University, West Lafayette, IN 47906*

⁴*Department of Computer and Electrical Engineering, UCSD, La Jolla, CA 92093*

(Dated: December 2, 2024)

PACS numbers: 74.78.Na, 74.25.Fy, 74.25.Ha, 74.40.+k

The definition of τ_{GL} should read $\tau_{GL} = (\pi/8)[\hbar/k_B(T_c - T)]$.

An inadvertent error in fitting to the magneto-resistance of the Al wires led to an underestimate of the wire widths and cross sections [2]. The revised width/cross section for the Al wires s1 (10 μm long) and s2 (100 μm long) are respectively: 11.4 nm /130 nm² and 7.5 nm/58 nm² roughly an increase of 40 % in width and factor of 2 in cross section. The wire widths have an error of $\pm 10\%$, and the cross section error is $\pm 20\%$. The revised sample parameters are listed in the revised Table I. Note that the wire length, L, and normal state resistance, R_N , remain unchanged.

The dependence of the free-energy barrier ΔF on the cross sectional area A is contained in the quantity L/R_N [3], removing any explicit dependence on A . Thus, the revised quantities, including A , are not used in the main analysis, and do not affect the main conclusion of the paper. The only notable effect is that the agreement between the fitted coherence length ξ_c and the calculated ξ now occurs at the boundary of the error bars. Note that the error on ξ_c is 15%. The fitted values for $\Delta F(H = 0, T = 0)$ and $\xi_c(H = 0, T = 0)$ (135 nm), combined with the revised A , yield a thermodynamic critical field $H_{th}(H = 0, T = 0) \approx 0.0096$ T (96 Oersted), close to the known value of 0.0105 T (105 Oersted) for bulk aluminum.

- [1] F. Altomare *et al.*, Appl. Phys. Lett. **86**, 172501 (2005).
- [2] F. Altomare *et al.*, submitted to App. Phys. Lett.
- [3] C. N. Lau *et al.*, Phys. Rev. Lett. **87**, 217003 (2001).

	L	w	t	R_N	ρ	l_e	ξ	J_c (0.35 K)
	μm	nm	nm	$k\Omega$	$\mu\Omega\text{cm}$	nm	nm	$10^5 A/\text{cm}^2$
s1	10	11.4	11.4	8.3	10.7	3.7	65	5.8
s2	100	7.5	7.7	86.4	5.0	7	90	7.2

TABLE I: Parameters for sample s1 and s2. The parameters L (length), w (width), t (thickness), R_N (normal state resistance), ρ (resistivity), l_e (mean free path), ξ (GL coherence length), and J_c (critical current density), for the two samples s1 and s2. w, t, ρ and l_e have been deduced following the analysis in Altomare et al.[1] based on magnetoresistance measurements. ξ was calculated using $\xi = 0.85\sqrt{\xi_0 l_e}$ where $\xi_0 = 1600$ nm is the GL superconducting coherence length.

Evidence for Macroscopic Quantum Tunneling of Phase Slips in Long One-Dimensional Superconducting Al Wires

Fabio Altomare, Albert M. Chang, Michael R. Melloch, Yuguang Hong, and Charles W. Tu

1. POWER LAW

An alternative fit to the V-I curves, distinct from the GIO(\equiv GIO+LAMH) fit (see text and Figs. 2(a)-(b) of main manuscript), is performed using the power law dependence proposed for quantum phase slips [1]:

$$V = V_S + K \cdot (I/I_k)^\nu \quad (1)$$

where $V_S = R_S I$ is due to the series resistance R_S , and K , I_k are appropriate coefficients. These fits are indistinguishable from the best fits with the GIO model and will not be reproduced here. The exponent ν is plotted as a function of the magnetic field H in Fig. E1, and is obtained from the V-I curves at different temperatures in Figs. 2(a)-(b) and 3 (main manuscript) and from additional H that are not shown. The large exponent value (≥ 3.2) and the rapid decrease of ν with increasing H is consistent with naive estimates based on the theoretical model.

Furthermore, it is also possible to account for the observed linear resistance versus T behavior with a power law dependence on the temperature: $R_{KL} = K_1 T^{\nu-1}$. Theory[1, 2] predicts that the power-law exponent ν in the R

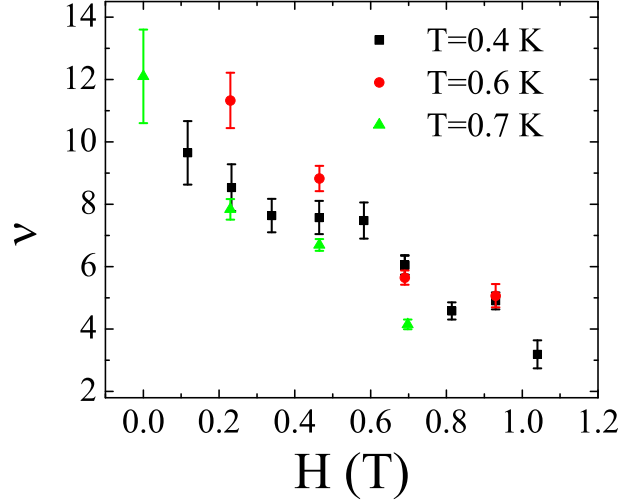


FIG. E1: The exponent ν , extracted from the fit of the V-I curves to the power law expression, has been plotted as function of the magnetic field. Different symbols correspond to V-I curves at different temperatures.

versus T dependence and in the V-I curves should be identical at each magnetic field. However, K_1 is predicted only under special limiting conditions. The fitting therefore necessitates the addition of K_1 as a fitting parameter. In doing so, the fitting becomes less restrictive.

2. DETAILS ON THE SUBTRACTION OF THE SERIES RESISTANCE

In the raw data for the 4-terminal, linear resistance versus temperature trace for sample s2 measured at $H = 0$ T, the resistance decreases precipitously from its normal state value, $R_N = 86\text{k}\Omega$ ($\gg R_q = h/4e^2 \approx 6.45\text{k}\Omega$), through the superconducting transition and saturates below 0.75 K at $47 \pm 4 \Omega$. This saturated value of the resistance is due to the pads and is measured in series with the nanowire. There are two contributions to the series resistance from each pad: one from an Au/Ti region without aluminum (Al) coverage which remains after the final aluminum evaporation (47Ω), and the other from the covered Al/Au/Ti region (0Ω when superconducting, and $\approx 423 \Omega$ when normal). The superconducting-to-normal (S-N) transition of the Al/Au/Ti pad regions as a function of the magnetic field H is shown in the inset of Fig. 1(a) in the main manuscript for several temperatures. It is indicated by the resistive jump at $H \sim \pm 0.1$ T. To confirm that the pad is responsible for this jump, separate two terminal measurement was performed for each pad, and in addition a different sample with the same Al/Au/Ti trilayer pad geometry, but connected to a wide Al wire, was also measured. In both cases a similar jump was observed in the resistance near $H \sim \pm 0.1$ T. At 0.34 K, the total pad resistance becomes independent of H above $H \approx 0.35$ T, having attained the full normal state value of $\approx 470 \Omega$. Above this field, this normal state value is also temperature independent. To extract the resistance of the nanowire, we subtract this resistance of 470Ω from the R vs. T raw data traces when $H \geq 0.465$ T, while for $H \leq 0.03$ T we subtract 47Ω instead, as the Al/Au/Ti regions become superconducting below ≈ 1 K and no longer contribute to the series resistance. The resultant traces are plotted in Fig. 1(a) of the main manuscript.

3. F-TEST

In the nonlinear voltage due to the thermal activation of phase slips (TAPS), $V_{TAPS} = I_0 R_{LAMH} \sinh(I/I_0)$ (Eq. (1b) main manuscript), the current scale $I_0 = 4ek_B T/h$ does not depend on the magnetic field H . However in the nonlinear voltage due to quantum tunneling of phase slips (QTPS), $V_{QTPS} = I_{GIO} R_{GIO} \sinh(I/I_{GIO})$ (Eq. (3) main manuscript), the current scale $I_{GIO} = 2e/(\pi\tau_{GL}a_{GIO})$ does depend on H through $\tau_{GL} = (\pi/8)[\hbar/k_B(T-T_c(H))]$.

Both $T_c(H)$ and a_{GIO} (in I_{GIO}) are deduced from fits to the linear R versus T traces and their values are presented in Fig. 4(a) and the text of the main manuscript, respectively.

In the measured voltage-current (V-I) curves the importance of TAPS was tested by fitting the experimental curves to $V = V_{TAPS} + V_S$. The series voltage $V_S = R_S I$ represents the contribution from ohmic-like resistances in series with the superconducting wire. To account for the contribution from the quantum tunneling of phase slips (QTPS), a V_{QTPS} term is added. The total QPS (\equiv QTPS + TAPS) contribution is given by $V = V_{QTPS} + V_{TAPS} + V_S$. The fitting parameters for the TAPS contribution without QTPS are R_{TAPS} and R_S [3]. For the QPS fit including QTPS, a third parameter R_{QTPS} is added. Note that to distinguish the fitting parameters from the theoretical ones, we refer to R_{TAPS} (R_{QTPS}) as the TAPS (QTPS) resistance extracted from the fits to the V-I curves, and to R_{LAMH} (R_{GIO}) as the theoretically calculated values (see Eqs. 1(a), 1(b), 2, and 3 in the main manuscript). As can be seen in Fig. 2(b) (main manuscript), the QPS fits are of good quality while the TAPS fits are much poorer. To quantitatively compare the two different fitting models, the statistical F-test[4] on chi-squares was applied to the random variable $F(n, m) = [(\chi_{QPS}^2 - \chi_{TAPS}^2)/\chi_{QPS}^2]/[(df_{QPS} - df_{TAPS})/df_{QPS}]$. Here $n = df_{QPS} - df_{TAPS}$, $m = df_{QPS}$ with df the number of degree of freedom, in the model under exam, defined by $df = N - p$, where N is the number of points and p the number of fitting parameter in the model, and χ_{QPS}^2 (χ_{TAPS}^2) represents the chi-square obtained by fitting the experimental data to the QPS (TAPS) model: $\chi^2(a_1 \cdots a_n) = \frac{1}{df} \sum [y_i - f(x_i, a_1 \cdots a_n)]$, with y_i and x_i the experimental data and $a_1 \cdots a_n$ fitting parameters. The F-test is useful for comparing two fitting expressions which belong to the same family of related expressions but one with more fitting parameter(s) than the other.

To accept the QPS and refuse the TAPS model with a confidence level exceeding 99%, $F(n, m)$ has to exceed the criterion for an integrated probability of 99% in the $F(n, m)$ distribution with n and m degrees of freedom. The F-test indicates that for the low temperature traces ($T/T_c \lesssim 0.5$) displayed in Fig.2(b) (main manuscript) as well as for all experimental V-I curves in Figs. 3 (main manuscript), the QPS model is preferred[5] with a confidence level greater than 99.99%. For example, for the traces in Fig. E2 (from Fig. 3(a) of the main manuscript), with: $n=1$, $m=89$, $\chi_{TAPS}^2 = 1.13E - 11$, $\chi_{QPS}^2 = 1.82E - 12$, we obtain that the likelihood in favor of the QPS model is basically 100% (actual numerical value $1 - 2.8 \times 10^{-13}$). Moreover, the excellent QTPS fits (no TAPS term) presented in Fig.3(a)-(c) (main manuscript) indicate that TAPS does not contribute in the low temperature limit ($T/T_c \lesssim 0.5$).

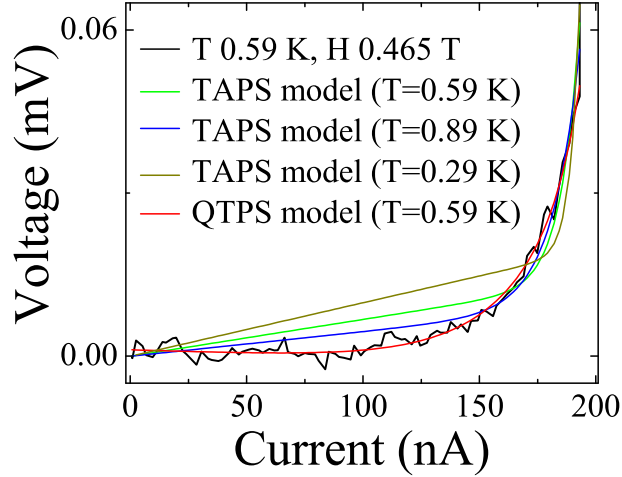


FIG. E2: (Color) Even by increasing the temperature by as much as 50% the TAPS model does not properly reproduce the experimental data as well as the QPS model (shown here for $T=0.59$ K and $H=0.465$ T). Reducing the temperature makes the fit even worse. The traces are displayed after subtracting the linear background contribution due to the series resistance.

4. ESTIMATE OF SELF-HEATING

In this section of the EPAPS we will show that any heating effect that may arise from the non-negligible power level dissipated in the superconducting wire, has minimal effects in the analysis of the nonlinear V-I curves of Fig. 2(a)-(b) and 3 (main manuscript) below the critical current I_C ($I < I_C$) and can be neglected, without loss of generality, in our fitting procedure. We will also show that it is reasonable to attribute the dominant thermal conduction to the lattice conduction of the InP ridge. After providing some preliminary details, we will show that, at a power of 15 pW dissipated through the nanowire and at a bath temperature $T_{bath}=0.4$ K, this self-heating would increase the wire temperature (T_w) to no more than 0.48 K (a relative change in temperature $\Delta T/T \lesssim 20\%$). Additionally, this temperature rise decreases with increasing bath temperature, due to increased thermal conduction of the InP ridge on which the nanowire sits, and, under the same assumptions, at $T=0.6$ K the relative change in temperature would be $\Delta T/T \lesssim 4\%$ and at $T=0.7$ K $\Delta T/T \lesssim 2.3\%$: this change in temperature alone, which does not depend on the magnetic field, cannot account for the observed non-linearity in the V-I. Our situation is in direct contrast with the results presented in other works where the superconducting wire was fabricated on suspended nanotubes[6, 7] and therefore lacked a direct thermal link to the substrate aside from the wire itself, for which, the electron thermal conductivity deduced from the electrical conductivity via the Wiedemann-Franz relation, was the dominant (but inadequate) means for thermal conduction. In particular, in the work of Johannson et al., heating seriously limits

the range of viable currents at their measuring temperature (~ 10 mK, much lower than in the present work). The two systems, however, cannot be directly compared because in the suspended nanotube geometry, the only additional cooling effect, beyond the electric thermal conduction, is due to the ^3He bath which is negligible because of the Kapitza boundary resistance. In our case the InP ridge, on which the wire is fabricated, readily thermalizes with the wafer; this in turn, because of its large (compared to the nanowire and the ridge) physical size ($0.5\text{ mm} \times 1.5\text{ mm} \times 2\text{ mm}$) is not affected by the Kapitza boundary resistance and can be efficiently cooled by the bath. We will demonstrate that, a) assuming a constant effective wire temperature (T_w), but higher than the bath temperature (T_{bath}), the TAPS theory still cannot properly reproduce the experimental data; b) the small increase in temperature we estimate, and the associated increase in resistance, is not nearly sufficient to explain the observed non linearity and, even by modifying our fitting procedure so as to include this temperature change into a temperature dependent coefficient, the TAPS model does not adequately describe the experimental data. On the other hand, the QPS ($\equiv \text{QTPS} + \text{TAPS}$) model fits the data well at all temperatures and fields examined. We would like to point out that at $T/T_c \lesssim 0.5$, which will be the main focus of this section, in the QPS model V_{TAPS} is negligible with respect to V_{QTPS} . Therefore, in the following we will refer equivalently to “QPS model” or to “QTPS model”.

The first point (a) is readily proven in Fig. E2 where the experimental data (for a representative trace displayed in Fig. 3(a) of the main paper) are fitted with the TAPS theory by changing the temperature by as much as 50%: the agreement between the TAPS model and the experimental data is still poor when compared to the QPS model.

Regarding the second point (b), we make the following observations to render the discussion more quantitative:

- 1) The power dissipated in the wire can be deduced from Fig. 2(a)-(b) using $V \cdot I = R \cdot I^2$ after subtracting the contribution due to the pads — $50\text{ }\Omega$ at $H=0\text{ T}$ and $470\text{ }\Omega$ at $H \geq 0.465\text{ T}$. Immediately before switching from the superconducting state to the normal state, the power dissipated in the wire (at all fields considered) is in the range $P \approx 5\text{-}15\text{ pW}$. To see that the electronic thermal contribution alone is not sufficient to cool the wire, as pointed out by referee A, we use a simple estimate based on the Wiedemann-Franz law and the heat diffusion equation ($\dot{Q} = A\kappa\nabla T$), with A the cross sectional area of the wire, κ the thermal conductivity and ∇T the temperature gradient, to find that, at $T=0.5\text{ K}$, it would produce an increase in temperature of several kelvin: an entirely inaccurate scenario, since the nanowire still exhibits a non-zero critical current, and therefore the effective wire temperature is smaller than the critical temperature ($T_c \sim 1.7\text{ K}$). This can be seen most dramatically in the V-I curve in the down sweep of the current (Fig. E3, red curve), where the power in the wire, immediately before switching from the normal to the

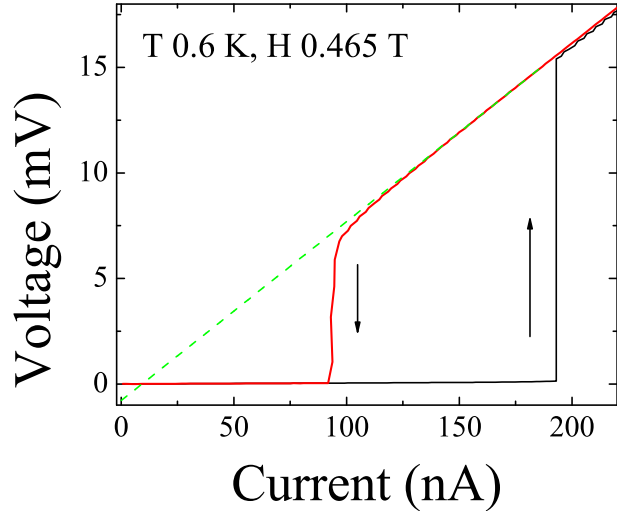


FIG. E3: (Color) V-I characteristic for the up (black) and down (red) sweep at $T=0.6$ K and $H=0.465$ T. The dashed line intersects the current axis at a finite current indicating the presence of a nonzero average supercurrent.

superconducting state, is greater than 200 pW. If there were no additional channels, *i.e.* the InP ridge and substrate, to conduct away the heat generated by this large power, the temperature rise would be so huge ($\gtrsim 10$ K) that no transition from the normal to the superconducting state would be observed. In fact, based on the experimental data, even at these power levels, the wire temperature cannot be above the critical temperature because a nonzero average supercurrent still flows in the nanowire. This can be deduced by noticing that the extrapolation of the down sweep V-I intercepts the current axis at a finite value (a typical curve is shown in Fig. E3 for the V-I trace taken at $T=0.6$ K and $H=0.465$ T). While this does not exclude the possibility of a slight temperature rise, it clearly excludes a naive model of thermal conduction with dominant electron component, based on the Wiedemann-Franz law, which would yield a large change in temperature. Moreover, this failure implies that the above description does not adequately model the experimental situation.

2) Thermalization of the wire in the vertical direction (~ 6.1 nm), as opposed to along the wire through the pads can readily be achieved via electronic conduction. This means that heat can easily be transferred from the top to the bottom of the nanowire across the 6.1 nm distance (the farthest and closest to the ridge, respectively), and any difference in temperature quickly equilibrated. In fact, because of the large cross sectional $—100\ \mu\text{m} \times 5.25\ \text{nm}$ —surface area (versus $5.25\ \text{nm} \times 6.1\ \text{nm}$ cross section for thermal conduction along the nanowire), even for a very high power of $P \sim 300$ pW (which would render the wire normal) and $T=0.5$ K, by using the heat diffusion equation combined with the Wiedemann-Franz law, we obtain $\Delta T \lesssim 1 \cdot 10^{-5}$ K. Any heat generated in the wire, therefore, will

be quickly transferred to the InP ridge which (as it will be discussed later in detail) is the dominant mechanism for thermally anchoring the wire to the bath.

3) The crystal thermal conductivity (κ) of the InP ridge and the InP/GaAs substrate is *independent of the magnetic field* and $\kappa \propto C_v \lambda_{ph}$ where λ_{ph} is the phonon mean free path and $C_v \propto T^3$ is the specific heat. For the bulk InP/GaAs substrate the phonon mean free path is limited by boundary scattering while for the InP ridge is most likely cut off by the height of the ridge ($\sim 25\text{ nm}$). Since the ridge width is only $\sim 8\text{ nm}$ and is almost atomically flat, the reflection off the ridge walls is likely specular (note that the thermal wavelength at 1 K is $\approx 50\text{ nm}$). Only bulk phonons, however, will be effective in transferring the heat because surface defects and adsorbates will limit the heat transferred by surface phonons.

4) One of the biggest problems in thermally anchoring a sample at the bath temperature, in low temperature measurements, is the Kapitza boundary resistance, defined as

$$R_k = A\Delta T/\dot{Q} \quad (2)$$

where A is the contact area, ΔT the difference in temperature between the bath and the sample (nanowire in our case) and \dot{Q} the heat flow. Based on values for other typical metals[8], because of the small contact area between ^3He and the aluminum nanowire, the bath cannot properly cool the nanowire. On the other hand, the crystal size ($.5\text{ mm} \times 1.5\text{ mm} \times 2\text{ mm}$) is such that any thermal boundary resistance can be ignored. Additionally, given the typical lattice conductivity of good crystals (at $T=1\text{ K}$, $\kappa \approx 0.01 - 8\text{ W/K m}$)[9, 10] from the heat diffusion equation, at $P=10\text{ pW}$, the increase in temperature for the crystal would be $\Delta T \lesssim 1 \cdot 10^{-4}\text{ K}$. Based on the above discussion, since the aluminum nanowire exhibits superconducting behavior, even at power of the order of 200 pW or more (finite non-zero switching current), the temperature must still be below $T_c \sim 1.7\text{ K}$. Therefore there must be some channel that efficiently anchors the nanowire to the bath temperature: this channel is the InP ridge, directly connected to the crystal substrate.

Below we present a quantitative analysis of the temperature rise, at the relevant power levels of $P \lesssim 15\text{ pW}$, for the non-linear V-I curves for Figs. 2(b) and 3 of the main manuscript. We begin by noting that the change in resistance due to the heat is not sufficient in explaining the observed non linearity.

In fact, let us assume (this will be demonstrated later) that a power of 15 pW produces a relative increase in temperature of 20% at $T=0.4\text{ K}$, 4% at $T=0.6\text{ K}$ and 2.3% at $T=0.7\text{ K}$. Because of the temperature dependence of the resistance—*i. e.* it increases with increasing temperature as shown in Fig. 1(a) of the main paper, there will be

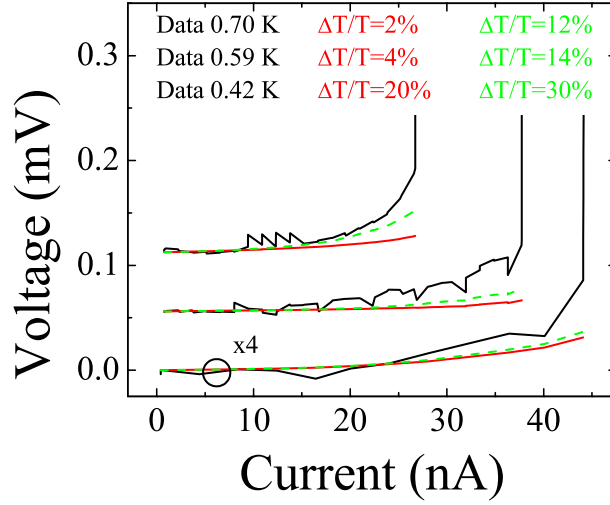


FIG. E4: (Color) Experimental V-I curves at $H=1.16$ T (black) and voltage drop across the superconducting nanowire calculated (red) up to the switching current by attributing the resistance change to the change in temperature (from bottom to top: $\Delta T/T = 20\%$ at $T=0.4$ K, $\Delta T/T = 4\%$ at $T=0.6$ K, $\Delta T/T = 2.3\%$ at $T=0.7$ K). The contribution due to the series resistance linear in the current has been subtracted and \bullet indicates curves multiplied by 4. Even after increasing our estimate by an additional 10% (green) the agreement is still poor. Curves are offset for clarity.

nonlinearity in the V-I characteristics. Any heating effect, however, will be independent of the magnetic field, so we can use the R vs. T (in the linear regime, Fig. 1(a) main manuscript) curve at $H=1.16$ T as a thermometer. This has the advantage of providing, in the temperature range of interest, the biggest change in resistance as function of the change in temperature. Since at this magnetic field the R vs. T data stops at $T \sim 0.48$ K, we linearly interpolated to obtain the data at the lowest temperature ($T=0.42$ K) by using the resistance in the corresponding V-I curve (at $H=1.16$ T) deduced in the limit of low current. Our results are shown in Fig. E4, where both experimental data and the voltage drop across the superconducting wire, calculated from the measured resistance with the change in temperature taken into account, are displayed after subtracting the contribution due to the series resistance which is linear in the current. Increasing the temperature by an additional 10% still does not reproduce the experimental data.

Therefore we can conclude that the major portion of the non-linearity cannot be attributed to self-heating.

From our discussion above, it is clear that assuming the wire temperature either does not change or changes within our estimate, the QPS model better describes the experimental data (see also Fig. E9). The only remaining task is to describe the method for obtaining the previously stated upper-bound estimates ($\Delta T/T = 20\%$ at $T=0.4$ K,

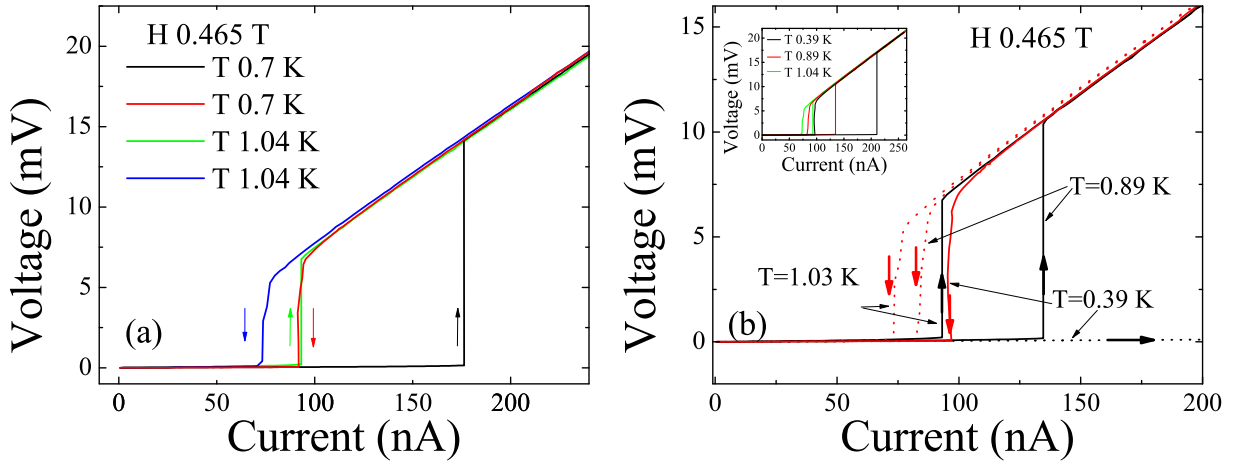


FIG. E5: (Color) $H=0.465$ T: (a) the down sweep at $T=0.7$ K has the same switching current as the up sweep at $T=1.04$ K: we conclude that at $T_{bath}=0.7$ K, a power level of $P \sim 600$ pW raises the wire temperature up to $T_w=1.04$ K. (b) At $T=0.39$ K, the down switching current is in between the up switching current at $T=1.04$ K and $T=0.89$ K. Linearly interpolating between these two values (see also Fig. E6), we obtain that at $T_{bath} \sim 0.39$ K, a power level $P \sim 644$ pW increases the wire temperature to $T_w=1.015$ K. The dotted curves refer to up and down sweep not relevant to this discussion. Inset: the full range of the V-I curves for the three different temperatures is shown.

$\Delta T/T = 4\%$ at $T=0.6$ K, $\Delta T/T = 2.3\%$ at $T=0.7$ K), which will involve using the position of the critical current jumps in the V-I curves themselves. Since self-heating will be particularly important at lower temperature, we will concentrate on the curves presented in Fig. 3 of the main manuscript for which the difference between the QPS (or the numerically equivalent QTPS) model and the TAPS model is the most apparent. Let us consider the situation depicted in Fig. E5(a). Here we show for magnetic field $H = 0.465$ T up (black) and down (red) sweeps at a bath temperature of $T=0.7$ K together with up (green) and down (blue) sweeps at $T=1.04$ K. It is evident that the current at which the nanowire switches from the normal to the superconducting state in a down-sweep at the bath temperature $T_{bath}=0.7$ K (red), with a corresponding dissipated power of $P \sim 600$ pW, coincides with the current at which the nanowire switches from the superconducting to the normal state at a bath temperature $T_{bath}=1.04$ K in an up-sweep (green). Since the switching positions overlap, we infer that at a bath temperature $T_{bath}=0.7$ K the wire temperature is not more than $T_w=1.04$ K, despite a power level $P \sim 600$ pW. This is equivalent to saying that, with a power $P \sim 600$ pW dissipated in the nanowire and at a bath temperature $T_{bath}=0.7$ K, the wire temperature rises to no more than $T_w=1.04$ K. This identification can be made because in the up-sweep, immediately before the transition from superconducting to normal state, the power level is sufficiently low that the wire temperature is very close to

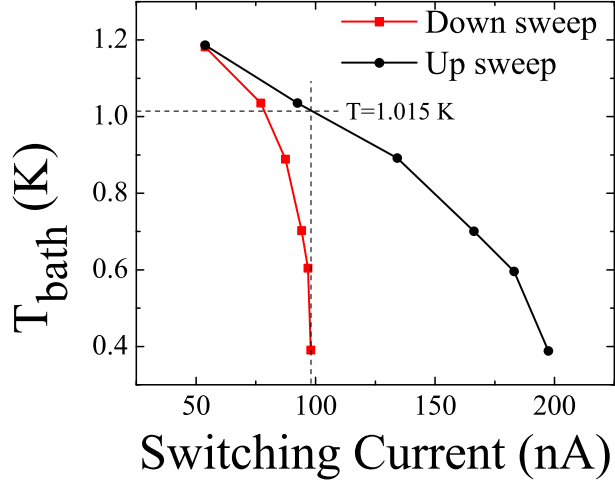


FIG. E6: At a field $H=0.465$ T, the bath temperature has been recorded as function of the up (black) and down (red) switching current. If we were to perform a measurement at $T=1.015$ K, the up switching current would be the same as the down switching current at $T=0.39$ K at a power given by the product $V \cdot I$ immediately before the transition from normal to superconducting state. By repeating the same procedure for the other fields of interest ($H=0, 0.7, 0.93$ T), we obtain the datapoints in Fig. E8 after allowing for some uncertainty in the value of the down switching current.

the bath temperature. The 600 pW dissipated power is estimated by multiplying the current and the voltage at the switching current in the down sweep (at $T_{bath}=0.7$ K) after subtracting the contribution due to the pads. For situations where a good match between different bath temperatures is not available, we linearly interpolate between two nearby temperatures to extract the value of interest (Fig. E6). An example is provided in Figs. E5(b) and E6. At a bath temperature $T_{bath}=0.39$ K, the wire temperature is $T_w=1.015$ K at a power level $P \sim 644$ pW (as before the power level is calculated from Fig. E5(b) after subtracting the pad contribution).

By following this procedure for all our datasets (representative V-I are shown in Fig. E7), we obtain, for every T_{bath} of interest ($T=0.4$ K, 0.6 K and 0.7 K), the corresponding T_w as a function of the power dissipated in the nanowire. This allows us to estimate, for the lattice temperatures mentioned above, the temperature rise due to the dissipated power: in particular we will be interested in the change in temperature at the power levels at which the wire switches from the superconducting to the normal state ($\lesssim 15$ pW).

Our results are displayed in Fig. E8 (a)–(c) where the scatter in the datapoints at a given magnetic field reflects the uncertainty in the exact determination of the switching current. In order to analyze these data, we model the InP ridge thermal conductivity as a 1-dimensional problem with $P = \dot{Q} = \kappa A \nabla T$. By integrating the heat diffusion equation along the ridge height direction and taking into account the the temperature dependence (T^3) of the crystal

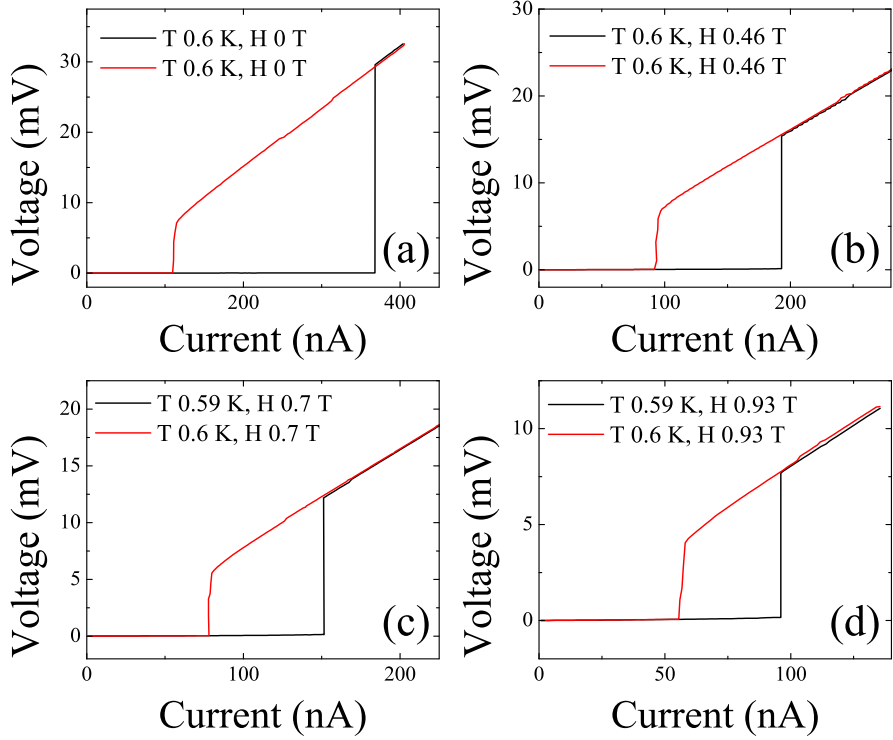


FIG. E7: (Color) (a)-(d): Typical V-I characteristics up (black) and down (red) sweep at $T \approx 0.6$ K at different magnetic field.

thermal conductivity, in a scenario where $\lambda_{ph} \sim const$, the expected behavior of T_w is $T_w = \sqrt[4]{P/C + T_{bath}^4}$ with C an appropriate constant that depends on the crystal and on the ridge geometry. Note that at zero power dissipated through the nanowire (and therefore zero current flowing), the aluminum nanowire must be in thermal equilibrium with the bath.

From the fit to this functional form, displayed in Fig. E8, we find that, for $P=15$ pW, $\Delta T/T = 20\%$ at $T=0.4$ K, $\Delta T/T = 4\%$ at $T=0.6$ K and $\Delta T/T = 2.3\%$ at $T=0.7$ K.

It must be noted that these values are an upper bound because we have neglected the temperature dependence of the phonon mean free path (which may behave like $\lambda_{ph} \propto 1/T$ [9]): the thermal conductivity, therefore, might have a weaker dependence on the temperature. By assuming $T_w = \sqrt[4]{P/C + T_{bath}^\alpha}$, with α a fitting parameter, we obtain $\alpha = 2.8$ in good agreement with our expectations ($\alpha \simeq 3$), which would further reduce our upper bound estimate for $\Delta T/T$. By incorporating the theoretical temperature dependence into R_{TAPS} and R_{QTPS} based on Eqs. (1a) and (2) of the main manuscript, and repeating the same analysis that has led to Fig. 3 (main manuscript), we obtained the fits shown in Fig. E9. It is apparent that the experimental curves can be adequately fitted only by the QPS (or numerically equivalent QTPS) expression. The quality of these fits is comparable to quality of those

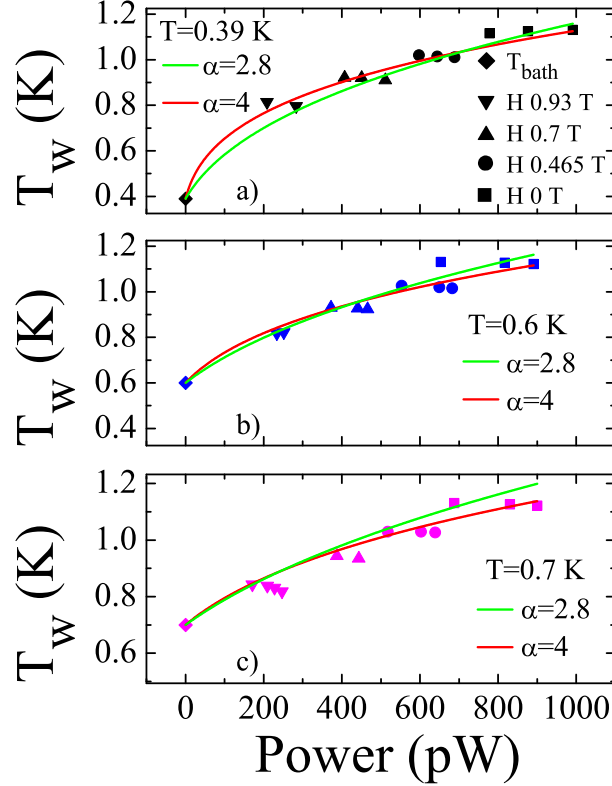


FIG. E8: (Color) Temperature reached by the superconducting nanowire at different power level and fit with the functional form discussed in the text for (a) $T_{bath}=0.4$ K, (b) $T_{bath}=0.6$ K, (c) $T_{bath}=0.7$ K: the scatter in the datapoints is due to the uncertainty in estimating the value of the current at which the nanowire switches from the normal to the superconducting state. Different symbol shapes indicate data points obtained at different fields.

shown in Fig. 3 of the main paper at $T_w = T_{bath}$. In Fig. E9 when fitting using the full expression for the QPS model ($V = V_{QTPS} + V_{TAPS} + V_S$), the contribution from V_{TAPS} is found to be negligible compared to V_{QTPS} , and F-test on the chi-squares for the datasets in Fig. E9 supports the QPS model with a confidence level exceeding 99.99%.

As an additional *independent check* on these temperature estimates, we point out that since the temperature increase is due solely to the power dissipated in the nanowire and should not depend on the applied magnetic field, we can use the V-I data at $H=1.16$ T to calculate a resistance (V/I) and a corresponding power level at each I , and then use the R vs. T curve to convert it to an effective, rough upper-bound temperature *assuming that any increase in resistance comes entirely from the temperature rise alone* and not from other sources of nonlinearity. By doing so we would obtain, for a power $P=15$ pW, $\Delta T/T = 31\%, 17\%, 17\%$ at $T=0.4, 0.6, 0.7$ K, respectively. By taking into account this estimated rise in temperature, larger than the more stringent estimate provided above, the TAPS theory still would not reproduce the data in Figs. 2(a)-(b) and 3 (main manuscript).

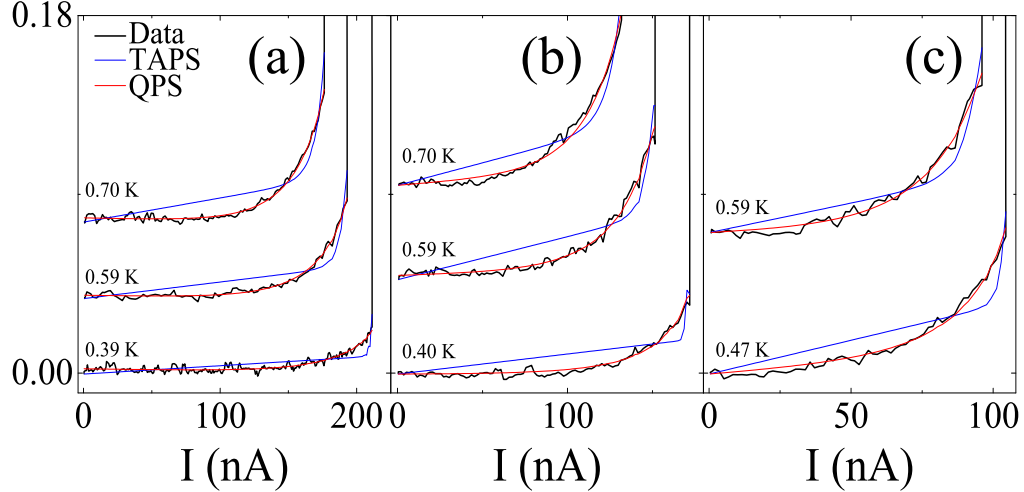


FIG. E9: (Color) The curves displayed in Fig. 3 (main paper) have been fit after including the theoretical temperature dependence in the fitting parameters R_{TAPS} and R_{QTPS} . As before, only the QPS (or numerically equivalent QTPS) model adequately fits the experimental data at all fields and temperatures. (The linear contribution due to the series resistance has been subtracted and the curves have been offset for clarity).

The last issue requiring examination is whether there is a possibility that the electron and phonons can become decoupled in the nanowire, which would prevent the transfer of heat from the electrons to the lattice, resulting in a situation where the electrons and lattice are no longer in equilibrium. The electron-phonon coupling follows a T^5 dependence in temperature, and is generally believed to be sufficiently strong at $T \geq 1\text{K}$. On the other hand, because of the T^5 dependence, a decoupling may arise below $T \sim 1\text{ K}$. We perform the following estimate to demonstrate that the reduced coupling at lower T does not cause a problem for heat transfer at power levels $\lesssim 15\text{ pW}$. To set the scale of the coupling we use the behavior at an electron temperature of 1 K for reference, where the electrons and phonons are expected to be in thermal equilibrium at high dissipated power. For a bath temperature of $\sim 0.4\text{ K}$ and electron temperature of 1 K, a dissipated power of 633 pW in the nanowire can be transferred to the lattice without difficulty (Fig. E8(a)). At the lower electron temperature of 0.48 K corresponding to our estimated upper bound of a 20% temperature rise at 0.4 K bath temperature, the electron-phonon coupling is reduced by a factor $(T/1\text{K})^5 = 0.0255$. The power level which would still allow the electrons and lattice to be in thermal equilibrium would thus be $633\text{ pW} \times 0.0255 = 16.14\text{ pW}$. The power relevant to the nonlinear V-I curves in our analysis ($\lesssim 15\text{ pW}$) is below this value. Therefore the reduction in coupling should not be problematic. This issue is even less relevant for the other two temperatures of interest presented in Figs. E8(b) and E8(c) (bath temperatures $> 0.4\text{ K}$ and electron

temperatures > 0.48 K).

In view of the evidence (both theoretical and experimental), we conclude that while slight increases in temperature cannot be ruled out for the power levels under consideration, the increases are inconsequential for the main results of the Letter and can be neglected. Thus, in fact we are observing a nonlinearity in the V-I characteristics which cannot be explained by the TAPS model, and which is instead compatible with the phenomenological model of QPS.



- [1] S. Khlebnikov, unpublished.
- [2] S. Khlebnikov and L. P. Pryadko, Phys. Rev. Lett. **95**, 107007 (2005).
- [3] For TAPS, we additionally imposed $V(I = 0^+) \geq 0$: marginally lower χ^2 could be obtained without this condition but this would have produced the unphysical results $V(I = 0^+) < 0$.
- [4] P. R. Bevington and K. D. Robinson, Data reduction and error analysis for the physical sciences (1992).
- [5] The F-test has been calculated using the (lower) value obtained relaxing the constraint $V(I = 0+) \geq 0$.
- [6] A. Rogachev, A. T. Bollinger, and A. Bezryadin, Phys. Rev. Lett. **94**, 017004 (2005).
- [7] A. Johansson, G. Sambandamurthy, N. Jacobson, D. Shahar, and R. Tenne, cond-mat/0505577 (2005).
- [8] G. L. Pollack, Rev. Mod. Phys. **41**, 48 (1969).
- [9] V. A. Osipov and S. E. Krasavin, Journal of Physics: Condensed Matter **10**, L639 (1998).
- [10] R. C. Zeller and R. O. Pohl, Phys. Rev. B **4**, 2029 (1971).